J. Math. Computer Sci., 41 (2026), 347–364

Online: ISSN 2008-949X

Journal of Mathematics and Computer Science

Journal Homepage: www.isr-publications.com/jmcs

On solving split variational inclusion problems with multi-inertial extrapolation and applications

Suparat Kesornprom[a,b], Papatsara Inkrong[c], Papinwich Paimsang[c], Nattawut Pholasa[c], Prasit Cholamjiak[c,*]

[a]Department of Mathematics, Faculty of Science, Chiang Mai University, Chiang Mai 50200, Thailand.

[b]Office of Research Administration, Chiang Mai University, Chiang Mai 50200, Thailand.

[c]School of Science, University of Phayao, Phayao 56000, Thailand.

Abstract

In this study, we address split variational inclusion problems in Hilbert spaces and introduce a new algorithm that combines multi-inertial extrapolation with a self-adaptive stepsize technique. The method is designed to enhance convergence performance while relaxing typical parameter constraints. Under suitable assumptions, we establish a weak convergence theorem. To validate the effectiveness of the approach, we apply it to real-world problems in image restoration and medical data classification.

Keywords: Split variational inclusion problems, multi-inertial extrapolation, weak convergence, image restoration, data classification.

2020 MSC: 47H09, 47H10, 47J05, 47J25, 49J40, 35A15.

1. Introduction

Let $\mathcal{H}_1$ and $\mathcal{H}_2$ be a real Hilbert spaces with the inner product $\langle \cdot, \cdot \rangle$ and the induced norm $\|\cdot\|$. Let $\mathcal{F} : \mathcal{H}_1 \to \mathcal{H}_2$ be a linear and bounded operator and $\mathcal{G}_1 : \mathcal{H}_1 \to 2^{\mathcal{H}_1}$ and $\mathcal{G}_2 : \mathcal{H}_2 \to 2^{\mathcal{H}_2}$ be multi-valued maximal monotone mappings. The split variational inclusion problem (SVIP) is to find $u^* \in \mathcal{H}_1$ such that $0_{\mathcal{H}_1} \in \mathcal{G}_1(u^*)$ and $0_{\mathcal{H}_2} \in \mathcal{G}_2(\mathcal{F}u^*)$. We set Ψ is a solution of SVIP such that $\Psi \neq \emptyset$. The SVIP is widely recognized as a general model that combines many important mathematical problems. These include the split common fixed-point problem [9, 12, 46], the split variational inequality problem [11, 48], the split zero problem [2, 5, 32, 36, 41], and the split feasibility problem [6, 10, 42, 51]. SVIP has also been applied in real-world situations such as signal processing, approximation theory, and data compression, showing its usefulness across theory and applications (see, e.g., [7, 15, 17, 33]). In addition, variational methods have been applied to study the existence of anti-periodic solutions for second-order impulsive differential inclusions. For instance, Heidarkhani et al. [23] established the existence of infinitely many anti-periodic solutions, while Hadjian and Heidarkhani [22] proved the existence of at least one non-trivial anti-periodic solution under suitable conditions.

*Corresponding author

Email addresses: suparat.ke@gmail.com (Suparat Kesornprom), papatsara.inkrong@gmail.com (Papatsara Inkrong), papinwich.ps@hotmail.com (Papinwich Paimsang), nattawat_math@hotmail.com (Nattawut Pholasa), prasit.ch@up.ac.th (Prasit Cholamjiak)

doi: 10.22436/jmcs.041.03.05

Received: 2025-07-17 *Revised:* 2025-08-25 *Accepted:* 2025-09-05

Let $\mathcal{G} : \mathcal{H} \to 2^{\mathcal{H}}$ be a set-valued maximal monotone operator. The resolvent operator $\mathcal{J}_\alpha^{\mathcal{G}} : \mathcal{H} \to \mathcal{H}$ is defined for any $\alpha > 0$ by

$$\mathcal{J}_\alpha^{\mathcal{G}}(u) = (I + \alpha\mathcal{G})^{-1}(u), \quad \forall u \in \mathcal{H},$$

where I denotes the identity operator on $\mathcal{H}$. It is well known that $\mathcal{J}_\alpha^{\mathcal{G}}$ is single-valued and firmly non-expansive. In 2011, Byrne et al. [8] introduced an iterative method for SVIP. Let $u_1 \in \mathcal{H}_1$ and $\{u_k\}$ be a sequence defined as follows:

$$u_{k+1} = \mathcal{J}_{\alpha_k}^{\mathcal{G}_1}(u_k - \lambda\mathcal{F}^*(I - \mathcal{J}_{\alpha_k}^{\mathcal{G}_2})\mathcal{F}u_k), \quad \forall k \geqslant 1,$$

where $\mathcal{F}^*$ is the adjoint of $\mathcal{F}$, $\lambda \in (0, 2/L)$, and L is the spectral radius of the operator $\mathcal{F}^*\mathcal{F}$. The authors established both weak and strong convergence results in Hilbert spaces. The variational inclusion problem (VIP) can be regarded as a special case of the SVIP. It seeks to find a point $u^* \in \mathcal{H}_1$ such that

$$0_{\mathcal{H}_1} \in \mathcal{G}_1(u^*), \tag{1.1}$$

where $\mathcal{G}_1 : \mathcal{H}_1 \to 2^{\mathcal{H}_1}$ is a set-valued mapping. The solution set of (1.1) is equivalently written as $\mathcal{G}_1^{-1}(0_{\mathcal{H}_1})$. To study this problem, Alvarez and Attouch [3] introduced the following inertial proximal algorithm. Let $u_0, u_1 \in \mathcal{H}_1$ and $\{u_k\}$ be a sequence defined by:

$$u_{k+1} = \mathcal{J}_{\alpha_k}^{\mathcal{G}_1}(u_k + \theta_k(u_k - u_{k-1})), \quad k \in N,$$

where $\{\theta_n\}$ is a sequence in $(0, \infty)$, $\{\theta_k\}$ is a sequence in $[0, 1)$ and $u_k + \theta_k(u_k - u_{k-1})$ is the one-step inertial extrapolation. This technique was introduced by Polyak [37] to acceleration process to solve a smooth convex minimization problem. The inertial extrapolation technique was originated from the heavy ball method of the second-order time dynamical system [2, 3].

In 2019, Poon and Liang [39] demonstrated that the use of a one-step inertial extrapolation may not always yield acceleration benefits when applied within the ADMM framework [13]. In particular, through the feasibility problem, it was shown that sequences generated by the one-step inertial fixed point iteration can converge more slowly than those produced by its non-inertial version. This observation indicates that one-step inertial extrapolation may fail to improve convergence speed. In contrast, two-step inertial fixed point methods have been shown to significantly improve convergence in terms of the number of iterations and computational time. Liang [30] further highlighted that employing multi-step inertial extrapolation, such as two-step inertial extrapolation given by: $u_k + \theta(u_k - u_{k-1}) + \gamma(u_{k-1} - u_{k-2})$, where $\theta > 0$ and $\gamma < 0$, can effectively overcome the limitations of the one-step extrapolation. This has motivated a line of research, including works by Polyak [38], Combettes and Glaudin [16], Dong et al. [18], Zhang et al. [52], Inkrong and Cholamjiak [24], Inkrong et al. [26], Iyiola and Shehu [27], Kankam et al. [28], Li et al. [29], Reich and Tuyen [43], and Zong et al. [53], all of which confirm the superior performance of multi-step inertial methods in accelerating optimization algorithms.

Recently, Dong et al. [18] introduced a modified multi-step inertial Mann-type iteration, which is defined by:

$$\begin{cases} z_k = u_k + \sum_{k \in \Omega_k} \theta_{s,k}(u_{k-s+1} - u_{k-s}), \\ w_k = u_k + \sum_{k \in \Omega_k} \eta_{s,k}(u_{k-s+1} - u_{k-s}), \\ u_{k+1} = (1 - \alpha_k)z_k + \alpha_k \mathcal{J}_\lambda^{\mathcal{G}}(w_k - \lambda\mathcal{F}w_k), \end{cases} \tag{1.2}$$

where $\Omega_k \subseteq \{0, 1, 2, \ldots, k-1\}$ for each $k \geqslant 1$, and the sequences $\{\theta_{s,k}\}$ and $\{\eta_{s,k}\}$ are taken from the set $(-1, 2]^{|\Omega_k|}$ for each $k \geqslant 2$. The authors proved that the sequence $\{u_k\}$ generated by (1.2) converges weakly to a solution of the variational inclusion problem.

In this paper, motivated by the works of Byrne et al. [8] and Dong et al. [18], we present an iterative method with the multi-step inertial term and the self adaptive stepsize for solving split variational inclusion problem. Moreover, a weak convergence theorem is established in the framework of real Hilbert spaces. Finally, we apply our algorithm to image restoration and data classification problem to support the implementation of the proposed method.

2. Preliminaries

This section outlines fundamental definitions and auxiliary results that are instrumental for the subsequent analysis. Throughout this paper, we employ the following notation conventions: the symbol $\rightharpoonup$ stands for weak convergence and the symbol $\to$ stands for strong convergence.

Let $\mathcal{T} : \mathcal{H} \to \mathcal{H}$ be an operator defined on a real Hilbert space $\mathcal{H}$. We define the following properties:

- The operator $\mathcal{T}$ is said to be **nonexpansive** if for all $u, v \in \mathcal{H}$, $\|\mathcal{T}u - \mathcal{T}v\| \leqslant \|u - v\|$.
- The operator $\mathcal{T}$ is said to be **firmly-nonexpansive** if it satisfies the inequality

$$\langle \mathcal{T}u - \mathcal{T}v, u - v\rangle \geqslant \|\mathcal{T}u - \mathcal{T}v\|^2, \quad \forall u, v \in \mathcal{H}.$$

  Moreover, it follows that if $\mathcal{T}$ is firmly-nonexpansive, then so is the mapping $I - \mathcal{T}$, where I is the identity operator [20].
- The operator $\mathcal{T}$ is said to be L**-Lipschitz continuous**, if there exists a constant $L > 0$ such that

$$\|\mathcal{T}u - \mathcal{T}v\| \leqslant L\|u - v\|, \quad \forall u, v \in \mathcal{H}.$$

- A set-valued mapping $\mathcal{G} : \mathcal{H} \to 2^{\mathcal{H}}$ is said to be **monotone** if, for all $u, v \in \mathcal{H}$, the following inequality holds: $\langle w - z, u - v\rangle \geqslant 0$, $\forall w \in \mathcal{G}u$ and $z \in \mathcal{G}v$. The graph of $\mathcal{G}$, denoted by $\text{graph}(\mathcal{G})$, is defined as $\text{graph}(\mathcal{G}) := \{(u, w) \in \mathcal{H} \times \mathcal{H} : w \in \mathcal{G}(u)\}$.
- A monotone mapping $\mathcal{G} : \mathcal{H} \to 2^{\mathcal{H}}$ is said to be **maximal** if its graph is not properly contained in the graph of any other monotone operator on $\mathcal{H}$. In other words, there is no monotone mapping whose graph strictly includes $\text{graph}(\mathcal{G})$.

Lemma 2.1 ([19]). *Let $\mathcal{C}$ be a nonempty closed convex subset of a real Hilbert space $\mathcal{H}$ and let $\mathcal{T} : \mathcal{C} \to \mathcal{C}$ be a nonexpansive mapping. If $u_k \rightharpoonup u \in \mathcal{C}$ and $\lim_{k\to\infty} \|u_k - \mathcal{T}u_k\| = 0$, then $u = \mathcal{T}u$.*

To proceed with the analysis of the SVIP, we introduce several key lemmas that will support our theoretical development. We denote the zero set of a set-valued mapping $\mathcal{G}$ by $\mathcal{G}^{-1}(0) = \{u \in \mathcal{H} : 0 \in \mathcal{G}u\}$. The domain of an operator $\mathcal{T}$ is denoted by $\mathcal{D}(\mathcal{T})$, and the set of fixed points of $\mathcal{T}$ is given by $\text{Fix}(\mathcal{T}) = \{u \in \mathcal{H} : u = \mathcal{T}u\}$.

Lemma 2.2 ([4]). *Let $\mathcal{H}$ be a real Hilbert space and let $\mathcal{G} : \mathcal{H} \to 2^{\mathcal{H}}$ be a set-valued maximal monotone mapping for each $u, v \in \mathcal{H}$, each $w \in \mathcal{G}^{-1}(0)$, and each $\alpha > 0$, the following properties hold:*

(i) $\langle u - \mathcal{J}^{\mathcal{G}}_{\alpha}u, w - \mathcal{J}^{\mathcal{G}}_{\alpha}u\rangle \leqslant 0$;
(ii) $\|\mathcal{J}^{\mathcal{G}}_{\alpha}u - w\|^2 \leqslant \|u - w\|^2 - \|\mathcal{J}^{\mathcal{G}}_{\alpha}u - u\|^2$;
(iii) $\|\mathcal{J}^{\mathcal{G}}_{\alpha}u - \mathcal{J}^{\mathcal{G}}_{\alpha}v\|^2 \leqslant \langle \mathcal{J}^{\mathcal{G}}_{\alpha}u - \mathcal{J}^{\mathcal{G}}_{\alpha}v, u - v\rangle$.

Lemma 2.3 ([14, 31, 40]). *Let $\mathcal{H}$ be a real Hilbert space and let $\mathcal{G} : \mathcal{H} \to 2^{\mathcal{H}}$ be a set-valued maximal monotone mapping. Then,*

(i) *for any $\alpha > 0$, the resolvent $\mathcal{J}^{\mathcal{G}}_{\alpha}$ is a single-valued and firmly nonexpansive mapping;*
(ii) $\mathcal{D}(\mathcal{J}^{\mathcal{G}}_{\alpha}) = \mathcal{H}$ *and* $\text{Fix}(\mathcal{J}^{\mathcal{G}}_{\alpha}) = \{u \in \mathcal{D}(\mathcal{G}) : 0 \in \mathcal{G}u\}$;
(iii) *for all $u \in \mathcal{H}$ and $0 < \alpha \leqslant \gamma$, we have $\|u - \mathcal{J}^{\mathcal{G}}_{\alpha}u\| \leqslant \|u - \mathcal{J}^{\mathcal{G}}_{\alpha}u\|$;*
(iv) *if $\mathcal{G}^{-1}(0) \neq \emptyset$, then for each $u \in \mathcal{H}$, each $u^* \in \mathcal{G}^{-1}(0)$, and each $\alpha > 0$, it holds that $\|u - \mathcal{J}^{\mathcal{G}}_{\alpha}u\|^2 + \|\mathcal{J}^{\mathcal{G}}_{\alpha}u - u^*\|^2 \leqslant \|u - u^*\|^2$;*
(v) *if $\mathcal{G}^{-1}(0) \neq \emptyset$, then for each $u \in \mathcal{H}$, each $w \in \mathcal{G}^{-1}(0)$, and each $\alpha > 0$, we have $\langle u - \mathcal{J}^{\mathcal{G}}_{\alpha}u,\ \mathcal{J}^{\mathcal{G}}_{\alpha}u - w\rangle \geqslant 0$.*

We next present a lemma that describes the solution structure of the SVIP by relating it to the fixed point properties of the resolvent operator derived from a maximal monotone mapping.

Lemma 2.4 ([14]). *Let $\mathcal{H}_1$ and $\mathcal{H}_2$ be real Hilbert spaces, and let $\mathcal{F} : \mathcal{H}_1 \to \mathcal{H}_2$ be a bounded linear operator. Suppose $\alpha > 0$ and let $\mathcal{G} : \mathcal{H}_2 \to 2^{\mathcal{H}_2}$ be a set-valued maximal monotone mapping. Define a mapping $\mathcal{T} : \mathcal{H}_1 \to \mathcal{H}_1$ by $\mathcal{T}u := u - \mathcal{F}^*(I - \mathcal{J}^{\mathcal{G}}_{\alpha})\mathcal{F}u$ for each $u \in \mathcal{H}_1$. Then, the following inequalities hold for all $u, v \in \mathcal{H}_1$:*

(i) $\|(I-J_\alpha^G)\mathcal{F}u-(I-J_\alpha^G)\mathcal{F}v\|^2 \leqslant \langle \mathcal{F}u-\mathcal{F}v,\ u-v\rangle$;
(ii) $\|\mathcal{F}^*(I-J_\alpha^G)\mathcal{F}u-\mathcal{F}^*(I-J_\alpha^G)\mathcal{F}v\|^2 \leqslant \|\mathcal{F}\|^2\cdot\langle \mathcal{F}u-\mathcal{F}v,\ u-v\rangle$.

Lemma 2.5 ([14]). *Let $\mathcal{H}_1$ and $\mathcal{H}_2$ be real Hilbert spaces and $\mathcal{F}:\mathcal{H}_1\to\mathcal{H}_2$ be a bounded linear operator. Let $\alpha>0$, $\lambda>0$, and suppose that $G_1:\mathcal{H}_1\to 2^{\mathcal{H}_1}$ and $G_2:\mathcal{H}_2\to 2^{\mathcal{H}_2}$ be set-valued maximal monotone mappings. Then for any $u^*\in\mathcal{H}_1$, the following statements hold:*

(i) *if u^* is a solution of the SVIP, then $J_\alpha^{G_1}(u^*-\lambda\mathcal{F}^*(I-J_\alpha^{G_2})\mathcal{F}u^*)=u^*$.*
(ii) *if the solution set of the SVIP is nonempty and $J_\alpha^{G_1}(u^*-\lambda\mathcal{F}^*(I-J_\alpha^{G_2})\mathcal{F}u^*)=u^*$, then u^* is a solution of the SVIP.*

The following lemmas are essential for convergence analysis.

Lemma 2.6 ([25]). *Let $s\in\{1,2,\dots,b\}$ for some $b\in N$. Suppose that the initial values $\Gamma_{1-b},\Gamma_{2-b},\dots,\Gamma_0$ be non-negative real numbers. Let $\{\Gamma_k\}_{k=1}^\infty$ and $\{\theta_{s,k}\}_{k=1}^\infty$ be non-negative real sequences. Assume that the following holds:*

$$\Gamma_{k+1}\leqslant\Gamma_k+\sum_{k=1}^{b}(\Gamma_{k-s+1}+\Gamma_{k-s})\theta_{s,k},\quad k\in N.$$

Then, the sequence $\{\Gamma_k\}$ satisfies $\Gamma_{k+1}\leqslant\mathcal{M}\cdot\prod_{j=1}^{k}(1+2\theta_{1,j}+2\theta_{2,j}+\cdots+2\theta_{b-1,j}+2\theta_{b,j})$, $k\in N$, where $\mathcal{M}=\max\{\Gamma_{1-b},\Gamma_{2-b},\dots,\Gamma_0,\Gamma_1\}$. Moreover, if $\sum_{k=1}^\infty\theta_{s,k}<+\infty$ for each $s\in\{1,2,\dots,b\}$, then the sequence $\{\Gamma_k\}$ is bounded.

Lemma 2.7 ([35]). *Let $\{b_k\}$, $\{\tau_k\}$ and $\{a_k\}$ be sequences of non-negative real numbers satisfying $b_{k+1}\leqslant(1+a_k)b_k+\tau_k$, $k\geqslant 1$. If $\sum_{k=1}^\infty a_k<+\infty$ and $\sum_{k=1}^\infty\tau_k<+\infty$, then $\lim_{k\to\infty}b_k$ exists.*

Lemma 2.8 ([34]). *Let Ψ be a subset of a real Hilbert space $\mathcal{H}$, and let $\{u_k\}\subseteq\mathcal{H}$ be a sequence satisfying the following conditions:*

(i) *for every $u^*\in\Psi$, $\lim_{k\to\infty}\|u_k-u^*\|$ exists;*
(ii) *every weak cluster point of $\{u_k\}$ belongs to Ψ.*

Then the sequence $\{u_k\}$ converges weakly to a point in Ψ.

3. Main results

In this section, we propose a multi-inertial proximal method combined with a self-adaptive stepsize strategy for solving the split variational inclusion problem in real Hilbert spaces. A weak convergence theorem is established under mild assumptions. Before presenting the proposed method, we first assume that the following conditions hold.

(C1) The solution set of the SVIP is nonempty, i.e., $\Psi\neq\emptyset$.
(C1) The mappings $\mathcal{F}:\mathcal{H}_1\to\mathcal{H}_2$ is a linear and bounded operator, and $\mathcal{F}^*$ is the adjoint operator of $\mathcal{F}$.
(C1) The mapping $G_1:\mathcal{H}_1\to 2^{\mathcal{H}_1}$ and $G_2:\mathcal{H}_2\to 2^{\mathcal{H}_2}$ are set-valued maximal monotone operators.

Algorithm 3.1 (Multi-inertial proximal method).
Initialization: Let $\mu_k\in(0,2)$, $d_k\in(0,1)$ and $\{\alpha_k\}_{k\in N}$ be a sequence in $(0,\infty)$. Fix an integer $b\in N$. For each $s\in\{1,2,\dots,b\}$, let $\{\theta_{s,k}\}_{k=1}^\infty$ be a sequence of non-negative real numbers. Let $u_{1-b},u_{2-b},\dots,u_0,u_1\in\mathcal{H}$. Let $\{u_k\}$ be defined by

$$\begin{cases} z_k=u_k+\sum_{s=1}^{b}\theta_{s,k}(u_{k-s+1}-u_{k-s}),\\ w_k=J_{\alpha_k}^{G_1}(z_k-\lambda_k\mathcal{F}^*(I-J_{\alpha_k}^{G_2})\mathcal{F}z_k),\\ u_{k+1}=w_k-\beta_k\mathcal{F}^*(I-J_{\alpha_k}^{G_2})\mathcal{F}w_k,\end{cases}$$

where the adaptive stepsizes λ_k and β_k are given by:

$$\lambda_k=\frac{\mu_k\|(I-J_{\alpha_k}^{G_2})\mathcal{F}z_k\|^2}{\|\mathcal{F}^*(I-J_{\alpha_k}^{G_2})\mathcal{F}z_k\|^2+d_k}\quad\text{and}\quad\beta_k=\frac{\mu_k\|(I-J_{\alpha_k}^{G_2})\mathcal{F}w_k\|^2}{\|\mathcal{F}^*(I-J_{\alpha_k}^{G_2})\mathcal{F}w_k\|^2+d_k}.$$

Theorem 3.2. *Let* $\{u_k\}$ *be defined by Algorithm 3.1. For each* $s \in \{1, 2, \ldots, b\}$, *if* $\sum_{k=1}^{\infty} \theta_{s,k} < +\infty$, $\lim_{k\to\infty} d_k = 0$ *and* $0 < \liminf_{k\to\infty} \mu_k \leqslant \limsup_{k\to\infty} \mu_k < 0$, *then*

(i) *for each* $u^* \in \Psi$, *we have* $\|u_{k+1} - u^*\| \leqslant M \cdot \prod_{j=1}^{k}(1 + 2\theta_{1,j} + 2\theta_{2,j} + \cdots + 2\theta_{b-1,j} + 2\theta_{b,j})$, *where* $M = \max\{\|u_{1-b} - u^*\|, \|u_{2-b} - u^*\|, \ldots, \|u_0 - u^*\|, \|u_1 - u^*\|\}$;

(ii) $\{u_k\}$ *converges weakly to a point in* Ψ.

Proof. Let $u^* \in \Psi$. Then $u^* \in \mathcal{G}_1^{-1}(0)$ and $\mathcal{F}u^* \in \mathcal{G}_2^{-1}(0)$. Since $\mathcal{J}_{\alpha_k}^{\mathcal{G}_2}\mathcal{F}z_k = \mathcal{F}z_k$, it follows that

$$\begin{aligned}\left\langle w_k - u^*, \mathcal{F}^*(I - \mathcal{J}_{\alpha_k}^{\mathcal{G}_2})\mathcal{F}w_k \right\rangle &= \left\langle w_k - u^*, \mathcal{F}^*(I - \mathcal{J}_{\alpha_k}^{\mathcal{G}_2})\mathcal{F}w_k - \mathcal{F}^*(I - \mathcal{J}_{\alpha_k}^{\mathcal{G}_2})\mathcal{F}u^* \right\rangle \\ &= \left\langle \mathcal{F}w_k - \mathcal{F}u^*, (I - \mathcal{J}_{\alpha_k}^{\mathcal{G}_2})\mathcal{F}w_k - (I - \mathcal{J}_{\alpha_k}^{\mathcal{G}_2})\mathcal{F}u^* \right\rangle \geqslant \|(I - \mathcal{J}_{\alpha_k}^{\mathcal{G}_2})\mathcal{F}w_k\|^2.\end{aligned} \tag{3.1}$$

Also, we have

$$\left\langle z_k - u^*, \mathcal{F}^*(I - \mathcal{J}_{\alpha_k}^{\mathcal{G}_2})\mathcal{F}z_k \right\rangle \geqslant \|(I - \mathcal{J}_{\alpha_k}^{\mathcal{G}_2})\mathcal{F}z_k\|^2. \tag{3.2}$$

Consider

$$\begin{aligned}\|u_{k+1} - u^*\|^2 &= \|w_k - \beta_k\mathcal{F}^*(I - \mathcal{J}_{\alpha_k}^{\mathcal{G}_2})\mathcal{F}w_k - u^*\|^2 \\ &= \|w_k - u^*\|^2 - 2\beta_k\langle w_k - u^*, \mathcal{F}^*(I - \mathcal{J}_{\alpha_k}^{\mathcal{G}_2})\mathcal{F}w_k\rangle + \beta_k^2\|\mathcal{F}^*(I - \mathcal{J}_{\alpha_k}^{\mathcal{G}_2})\mathcal{F}w_k\|^2.\end{aligned} \tag{3.3}$$

By Lemma 2.3 (ii), we get

$$\begin{aligned}\|w_k - u^*\|^2 &= \|\mathcal{J}_{\alpha_k}^{\mathcal{G}_1}(z_k - \lambda_k\mathcal{F}^*(I - \mathcal{J}_{\alpha_k}^{\mathcal{G}_2})\mathcal{F}z_k) - u^*\|^2 \\ &\leqslant \|z_k - \lambda_k\mathcal{F}^*(I - \mathcal{J}_{\alpha_k}^{\mathcal{G}_2})\mathcal{F}z_k - u^*\|^2 - \|w_k - (z_k - \lambda_k\mathcal{F}^*(I - \mathcal{J}_{\alpha_k}^{\mathcal{G}_2})\mathcal{F}z_k)\|^2 \\ &= \|z_k - u^*\|^2 - 2\lambda_k\langle z_k - u^*, \mathcal{F}^*(I - \mathcal{J}_{\alpha_k}^{\mathcal{G}_2})\mathcal{F}z_k\rangle + \lambda_k^2\|\mathcal{F}^*(I - \mathcal{J}_{\alpha_k}^{\mathcal{G}_2})\mathcal{F}z_k\|^2 \\ &\quad - \|w_k - z_k + \lambda_k\mathcal{F}^*(I - \mathcal{J}_{\alpha_k}^{\mathcal{G}_2})\mathcal{F}z_k\|^2.\end{aligned} \tag{3.4}$$

Replacing (3.1), (3.2), and (3.4) into (3.3), we get

$$\begin{aligned}\|u_{k+1} - u^*\|^2 &\leqslant \|z_k - u^*\|^2 - 2\lambda_k\langle z_k - u^*, \mathcal{F}^*(I - \mathcal{J}_{\alpha_k}^{\mathcal{G}_2})\mathcal{F}z_k\rangle + \lambda_k^2\|\mathcal{F}^*(I - \mathcal{J}_{\alpha_k}^{\mathcal{G}_2})\mathcal{F}z_k\|^2 - \|w_k \\ &\quad - z_k + \lambda_k\mathcal{F}^*(I - \mathcal{J}_{\alpha_k}^{\mathcal{G}_2})\mathcal{F}z_k\|^2 - 2\beta_k\langle w_k - u^*, \mathcal{F}^*(I - \mathcal{J}_{\alpha_k}^{\mathcal{G}_2})\mathcal{F}w_k\rangle + \beta_k^2\|\mathcal{F}^*(I - \mathcal{J}_{\alpha_k}^{\mathcal{G}_2})\mathcal{F}w_k\|^2 \\ &\leqslant \|z_k - u^*\|^2 - 2\lambda_k\|(I - \mathcal{J}_{\alpha_k}^{\mathcal{G}_2})\mathcal{F}z_k\|^2 + \lambda_k^2\|\mathcal{F}^*(I - \mathcal{J}_{\alpha_k}^{\mathcal{G}_2})\mathcal{F}z_k\|^2 \\ &\quad - \|w_k - z_k + \lambda_k\mathcal{F}^*(I - \mathcal{J}_{\alpha_k}^{\mathcal{G}_2})\mathcal{F}z_k\|^2 - 2\beta_k\|(I - \mathcal{J}_{\alpha_k}^{\mathcal{G}_2})\mathcal{F}w_k\|^2 + \beta_k^2\|\mathcal{F}^*(I - \mathcal{J}_{\alpha_k}^{\mathcal{G}_2})\mathcal{F}w_k\|^2 \\ &= \|z_k - u^*\|^2 - \frac{2\mu_k\|(I - \mathcal{J}_{\alpha_k}^{\mathcal{G}_2})\mathcal{F}z_k\|^2}{\|\mathcal{F}^*(I - \mathcal{J}_{\alpha_k}^{\mathcal{G}_2})\mathcal{F}z_k\|^2 + d_k}\|(I - \mathcal{J}_{\alpha_k}^{\mathcal{G}_2})\mathcal{F}z_k\|^2 \\ &\quad + \left(\frac{\mu_k\|(I - \mathcal{J}_{\alpha_k}^{\mathcal{G}_2})\mathcal{F}z_k\|^2}{\|\mathcal{F}^*(I - \mathcal{J}_{\alpha_k}^{\mathcal{G}_2})\mathcal{F}z_k\|^2 + d_k}\right)^2\|\mathcal{F}^*(I - \mathcal{J}_{\alpha_k}^{\mathcal{G}_2})\mathcal{F}z_k\|^2 \\ &\quad - \|w_k - z_k + \lambda_k\mathcal{F}^*(I - \mathcal{J}_{\alpha_k}^{\mathcal{G}_2})\mathcal{F}z_k\|^2 - \frac{2\mu_k\|(I - \mathcal{J}_{\alpha_k}^{\mathcal{G}_2})\mathcal{F}w_k\|^2}{\|\mathcal{F}^*(I - \mathcal{J}_{\alpha_k}^{\mathcal{G}_2})\mathcal{F}w_k\|^2 + d_k}\|(I - \mathcal{J}_{\alpha_k}^{\mathcal{G}_2})\mathcal{F}w_k\|^2 \\ &\quad + \left(\frac{\mu_k\|(I - \mathcal{J}_{\alpha_k}^{\mathcal{G}_2})\mathcal{F}w_k\|^2}{\|\mathcal{F}^*(I - \mathcal{J}_{\alpha_k}^{\mathcal{G}_2})\mathcal{F}w_k\|^2 + d_k}\right)^2\|\mathcal{F}^*(I - \mathcal{J}_{\alpha_k}^{\mathcal{G}_2})\mathcal{F}w_k\|^2 \\ &\leqslant \|z_k - u^*\|^2 - \frac{2\mu_k\left(\|(I - \mathcal{J}_{\alpha_k}^{\mathcal{G}_2})\mathcal{F}z_k\|^2\right)^2}{\|\mathcal{F}^*(I - \mathcal{J}_{\alpha_k}^{\mathcal{G}_2})\mathcal{F}z_k\|^2 + d_k} + \frac{\mu_k\left(\|(I - \mathcal{J}_{\alpha_k}^{\mathcal{G}_2})\mathcal{F}z_k\|^2\right)^2}{\|\mathcal{F}^*(I - \mathcal{J}_{\alpha_k}^{\mathcal{G}_2})\mathcal{F}z_k\|^2 + d_k}\end{aligned} \tag{3.5}$$

$$
\begin{aligned}
&- \|w_k - z_k + \lambda_k \mathcal{F}^*(I - \mathcal{J}_{\alpha_k}^{\mathcal{G}_2})\mathcal{F}z_k\|^2 - \frac{2\mu_k \left(\|(I - \mathcal{J}_{\alpha_k}^{\mathcal{G}_2})\mathcal{F}w_k\|^2\right)^2}{\|\mathcal{F}^*(I - \mathcal{J}_{\alpha_k}^{\mathcal{G}_2})\mathcal{F}w_k\|^2 + d_k} + \frac{\mu_k \left(\|(I - \mathcal{J}_{\alpha_k}^{\mathcal{G}_2})\mathcal{F}w_k\|^2\right)^2}{\|\mathcal{F}^*(I - \mathcal{J}_{\alpha_k}^{\mathcal{G}_2})\mathcal{F}w_k\|^2 + d_k} \\
&= \|z_k - u^*\|^2 - (2 - \mu_k)\mu_k \frac{\left(\|(I - \mathcal{J}_{\alpha_k}^{\mathcal{G}_2})\mathcal{F}z_k\|^2\right)^2}{\|\mathcal{F}^*(I - \mathcal{J}_{\alpha_k}^{\mathcal{G}_2})\mathcal{F}z_k\|^2 + d_k} \\
&\quad - \|w_k - z_k + \lambda_k \mathcal{F}^*(I - \mathcal{J}_{\alpha_k}^{\mathcal{G}_2})\mathcal{F}z_k\|^2 - (2 - \mu_k)\mu_k \frac{\left(\|(I - \mathcal{J}_{\alpha_k}^{\mathcal{G}_2})\mathcal{F}w_k\|^2\right)^2}{\|\mathcal{F}^*(I - \mathcal{J}_{\alpha_k}^{\mathcal{G}_2})\mathcal{F}w_k\|^2 + d_k}.
\end{aligned}
$$

Since $\mu_k \in (0,2)$, we have $\|u_{k+1} - u^*\| \leqslant \|z_k - u^*\|$. So, we obtain

$$
\begin{aligned}
\|u_{k+1} - u^*\| \leqslant \|z_k - u^*\| &= \left\| u_k + \sum_{s=1}^{b} \theta_{s,k}(u_{k-s+1} - u_{k-s}) - u^* \right\| \\
&\leqslant \|u_k - u^*\| + \sum_{s=1}^{b} \theta_{s,k} \|u_{k-s+1} - u_{k-s}\| \\
&\leqslant \|u_k - u^*\| + \sum_{s=1}^{b} \theta_{s,k}[\|u_{k-s+1} - u^*\| + \|u_{k-s} - u^*\|].
\end{aligned}
$$

By Lemma 2.6, we obtain

$$
\|u_{k+1} - u^*\| \leqslant \mathcal{M} \cdot \prod_{j=1}^{k}(1 + 2\theta_{1,j} + 2\theta_{2,j} + \cdots + 2\theta_{b-1,j} + 2\theta_{b,j}), \tag{3.6}
$$

where $M = \max\{\|u_{1-b} - u^*\|, \|u_{2-b} - u^*\|, \ldots, \|u_0 - u^*\|, \|u_1 - u^*\|\}$. By Lemma 2.6 and $\sum_{k=1}^{\infty} \theta_{s,k} < +\infty$, we obtain $\{u_k\}$ is bounded. So, we have $\sum_{s=1}^{b} \theta_{s,k} \|u_{k-s+1} - u_{k-s}\| < \infty$. Applying Lemma 2.7 in (3.6), it implies that $\lim_{k\to\infty} \|u_k - u^*\|$ exists.
Moreover, we have

$$
\begin{aligned}
\|z_k - u^*\|^2 &= \left\| u_k + \sum_{s=1}^{b} \theta_{s,k}(u_{k-s+1} - u_{k-s}) - u^* \right\|^2 + 2\left\langle u_k - u^*, \sum_{s=1}^{b} \theta_{s,k}(u_{k-s+1} - u_{k-s}) \right\rangle \\
&\leqslant \|u_k - u^*\|^2 + \left(\sum_{s=1}^{b} \theta_{s,k} \|u_{k-s+1} - u_{k-s}\| \right)^2 + 2\sum_{s=1}^{b} \theta_{s,k} \|u_k - u^*\| \|u_{k-s+1} - u_{k-s}\|.
\end{aligned} \tag{3.7}
$$

From (3.5) and (3.7), we get

$$
\begin{aligned}
\|u_{k+1} - u^*\|^2 \leqslant \|u_k - u^*\|^2 &+ \left(\sum_{s=1}^{b} \theta_{s,k} \|u_{k-s+1} - u_{k-s}\| \right)^2 + 2\sum_{s=1}^{b} \theta_{s,k} \|u_k - u^*\| \|u_{k-s+1} - u_{k-s}\| \\
&- (2 - \mu_k)\mu_k \frac{\left(\|(I - \mathcal{J}_{\alpha_k}^{\mathcal{G}_2})\mathcal{F}z_k\|^2\right)^2}{\|\mathcal{F}^*(I - \mathcal{J}_{\alpha_k}^{\mathcal{G}_2})\mathcal{F}z_k\|^2 + d_k} - \|w_k - z_k + \lambda_k \mathcal{F}^*(I - \mathcal{J}_{\alpha_k}^{\mathcal{G}_2})\mathcal{F}z_k\|^2 \\
&- (2 - \mu_k)\mu_k \frac{\left(\|(I - \mathcal{J}_{\alpha_k}^{\mathcal{G}_2})\mathcal{F}w_k\|^2\right)^2}{\|\mathcal{F}^*(I - \mathcal{J}_{\alpha_k}^{\mathcal{G}_2})\mathcal{F}w_k\|^2 + d_k}.
\end{aligned} \tag{3.8}
$$

From (3.8) and assumption of μ_k, we obtain

$$
\lim_{k\to\infty} \frac{\left(\|(I - \mathcal{J}_{\alpha_k}^{\mathcal{G}_2})\mathcal{F}z_k\|^2\right)^2}{\|\mathcal{F}^*(I - \mathcal{J}_{\alpha_k}^{\mathcal{G}_2})\mathcal{F}z_k\|^2 + d_k} = 0.
$$

It easy to check that $\{\|\mathcal{F}^*(I-\mathcal{J}_{\alpha_k}^{\mathcal{G}_2})\mathcal{F}z_k\|\}$ is bounded. Since $d_k \longrightarrow 0$, we get

$$\lim_{k\to\infty}\|(I-\mathcal{J}_{\alpha_k}^{\mathcal{G}_2})\mathcal{F}z_k\| = 0. \tag{3.9}$$

Also, we obtain

$$\lim_{k\to\infty}\|(I-\mathcal{J}_{\alpha_k}^{\mathcal{G}_2})\mathcal{F}w_k\| = 0. \tag{3.10}$$

From (3.9), we see that

$$\lambda_k\|\mathcal{F}^*(I-\mathcal{J}_{\alpha_k}^{\mathcal{G}_2})\mathcal{F}z_k\| = \frac{\mu_k\|(I-\mathcal{J}_{\alpha_k}^{\mathcal{G}_2})\mathcal{F}z_k\|^2}{\|\mathcal{F}^*(I-\mathcal{J}_{\alpha_k}^{\mathcal{G}_2})\mathcal{F}z_k\|^2+d_k}\|\mathcal{F}^*(I-\mathcal{J}_{\alpha_k}^{\mathcal{G}_2})\mathcal{F}z_k\| \ \to 0 \ \text{ as } \ k\to\infty. \tag{3.11}$$

From (3.8), we have

$$\lim_{k\to\infty}\|w_k - z_k + \lambda_k\mathcal{F}^*(I-\mathcal{J}_{\alpha_k}^{\mathcal{G}_2})\mathcal{F}z_k\| = 0. \tag{3.12}$$

By (3.11) and (3.12), it implies that

$$\begin{aligned}\|w_k - z_k\| &= \|w_k - z_k + \lambda_k\mathcal{F}^*(I-\mathcal{J}_{\alpha_k}^{\mathcal{G}_2})\mathcal{F}z_k - \lambda_k\mathcal{F}^*(I-\mathcal{J}_{\alpha_k}^{\mathcal{G}_2})\mathcal{F}z_k\| \\ &= \|w_k - z_k + \lambda_k\mathcal{F}^*(I-\mathcal{J}_{\alpha_k}^{\mathcal{G}_2})\mathcal{F}z_k\| + \|\lambda_k\mathcal{F}^*(I-\mathcal{J}_{\alpha_k}^{\mathcal{G}_2})\mathcal{F}z_k\| \ \to 0 \ \text{ as } \ k\to\infty.\end{aligned} \tag{3.13}$$

Observe that

$$\|z_k - u_k\| = \left\|u_k + \sum_{s=1}^{b}\theta_{s,k}(u_{k-s+1}-u_{k-s}) - u_k\right\| \leqslant \sum_{s=1}^{b}\theta_{s,k}\|u_{k-s+1}-u_{k-s}\| \ \to 0 \ \text{ as } \ k\to\infty. \tag{3.14}$$

From (3.13) and (3.14), we have $\lim_{k\to\infty}\|w_k - z_k\| = 0$. Also, from the definition of u_{k+1} and $\lim_{k\to\infty}\|(I-\mathcal{J}_{\alpha_k}^{\mathcal{G}_2})\mathcal{F}w_k\|$, we get $\lim_{k\to\infty}\|u_{k+1}-w_k\| = 0$. By Lemma 2.3 (i), (3.9), and (3.13), we have

$$\begin{aligned}\|\mathcal{F}w_k - \mathcal{J}_{\alpha_k}^{\mathcal{G}_2}w_k\| &\leqslant \|\mathcal{F}w_k - \mathcal{J}_{\alpha_k}^{\mathcal{G}_2}w_k - \mathcal{F}z_k + \mathcal{J}_{\alpha_k}^{\mathcal{G}_2}z_k\| + \|\mathcal{F}z_k - \mathcal{J}_{\alpha_k}^{\mathcal{G}_2}z_k\| \\ &\leqslant 2\|\mathcal{F}\|\|w_k - z_k\| + \|\mathcal{F}z_k - \mathcal{J}_{\alpha_k}^{\mathcal{G}_2}z_k\| \ \to 0 \ \text{ as } \ k\to\infty.\end{aligned}$$

By Lemma 2.3 (iii), we have

$$\|\mathcal{F}w_k - \mathcal{J}_{\alpha}^{\mathcal{G}_2}\mathcal{F}w_k\| \leqslant \|\mathcal{F}w_k - \mathcal{J}_{\alpha_k}^{\mathcal{G}_2}\mathcal{F}w_k\| \ \to 0 \ \text{ as } \ k\to\infty.$$

By Lemma 2.3 (i) and (3.9), we have

$$\|w_k - \mathcal{J}_{\alpha_k}^{\mathcal{G}_1}z_k\| = \|\mathcal{J}_{\alpha_k}^{\mathcal{G}_1}(z_k - \lambda_k\mathcal{F}^*(I-\mathcal{J}_{\alpha_k}^{\mathcal{G}_2})\mathcal{F}z_k) - \mathcal{J}_{\alpha_k}^{\mathcal{G}_1}z_k\| \leqslant \lambda_k\|\mathcal{F}^*\|\|(I-\mathcal{J}_{\alpha_k}^{\mathcal{G}_2})\mathcal{F}z_k\| \to 0 \ \text{ as } \ k\to\infty. \tag{3.15}$$

From (3.13) and (3.15), we obtain

$$\|z_k - \mathcal{J}_{\alpha_k}^{\mathcal{G}_1}z_k\| = \|z_k - w_k + w_k - \mathcal{J}_{\alpha_k}^{\mathcal{G}_1}z_k\| \leqslant \|z_k - w_k\| + \|w_k - \mathcal{J}_{\alpha_k}^{\mathcal{G}_1}z_k\| \ \to 0 \ \text{ as } \ k\to\infty.$$

Also by Lemma 2.3 (iii), we have

$$\|z_k - \mathcal{J}_{\alpha}^{\mathcal{G}_1}z_k\| \leqslant \|z_k - \mathcal{J}_{\alpha_k}^{\mathcal{G}_2}z_k\| \ \to 0 \ \text{ as } \ k\to\infty. \tag{3.16}$$

From (3.9) and (3.14), we obtain

$$\begin{aligned}\|\mathcal{F}u_k - \mathcal{J}_{\alpha}^{\mathcal{G}_2}\mathcal{F}u_k\| &\leqslant \|\mathcal{F}u_k - \mathcal{J}_{\alpha}^{\mathcal{G}_2}\mathcal{F}u_k - \mathcal{F}z_k + \mathcal{J}_{\alpha}^{\mathcal{G}_2}\mathcal{F}z_k\| + \|\mathcal{F}z_k - \mathcal{J}_{\alpha}^{\mathcal{G}_2}\mathcal{F}z_k\| \\ &\leqslant 2\|\mathcal{F}\|\|u_k - z_k\| + \|\mathcal{F}z_k - \mathcal{J}_{\alpha}^{\mathcal{G}_2}\mathcal{F}z_k\| \ \to 0 \ \text{ as } \ k\to\infty.\end{aligned} \tag{3.17}$$

From (3.14) and (3.16), we obtain

$$\begin{aligned}\|u_k - \mathcal{J}_{\alpha}^{\mathcal{G}_1}u_k\| &= \|u_k - z_k + z_k - \mathcal{J}_{\alpha}^{\mathcal{G}_1}z_k + \mathcal{J}_{\alpha}^{\mathcal{G}_1}z_k - \mathcal{J}_{\alpha}^{\mathcal{G}_1}u_k\| \\ &\leqslant \|u_k - z_k\| + \|z_k - \mathcal{J}_{\alpha}^{\mathcal{G}_1}z_k\| + \|\mathcal{J}_{\alpha}^{\mathcal{G}_1}z_k - \mathcal{J}_{\alpha}^{\mathcal{G}_1}u_k\| \ \to 0 \ \text{ as } \ k\to\infty.\end{aligned} \tag{3.18}$$

Since $\{u_k\}$ is bounded, there exists a subsequence $\{u_{k_i}\}$ of $\{u_k\}$ and $u^* \in \mathcal{H}_1$ such that $u_{k_i} \rightharpoonup u^*$. Given that $\mathcal{F}$ is a bounded linear operator, it follows that $\mathcal{F}u_{k_i} \rightharpoonup \mathcal{F}u^*$. Using (3.17), (3.18), Lemma 2.1 and Lemma 2.3 (iii), we deduce that $u^* \in \Psi$. Finally, by applying Lemma 2.8, we conclude that $\{u_k\}$ converges weakly to a point in Ψ. This completes the proof. □

4. Applications

4.1. Split feasibility problem

In this section, we connect the proposed method (Algorithm 3.1) to the Split Feasibility Problem (SFP), which involves finding a point $u^* \in \mathcal{H}_1$ satisfying

$$u^* \in \mathcal{C} \quad \text{and} \quad \mathcal{F}u^* \in \mathcal{Q}, \tag{4.1}$$

where $\mathcal{H}_1$ and $\mathcal{H}_2$ are real Hilbert spaces, $\mathcal{C} \subset \mathcal{H}_1$ and $\mathcal{Q} \subset \mathcal{H}_2$ are nonempty closed convex sets, and $\mathcal{F} : \mathcal{H}_1 \to \mathcal{H}_2$ is a bounded linear operator with adjoint $\mathcal{F}^*$. We denote Γ as a solution set of (4.1).

Let $\mathcal{H}$ be a Hilbert space and let $g : \mathcal{H} \to (-\infty, \infty]$ be a proper, lower semicontinuous, and convex function. The subdifferential of g, denoted by ∂g, is defined for each $u \in \mathcal{H}$ as:

$$\partial g(u) = \{w \in \mathcal{H} : g(u) + \langle w, v - u\rangle \leqslant g(v),\ \forall v \in \mathcal{H}\}.$$

Let $\mathcal{C}$ be a nonempty closed convex subset of $\mathcal{H}$, and ι_C be the indicator function of $\mathcal{C}$ defined by

$$\iota_{\mathcal{C}} u = \begin{cases} 0, & \text{if } u \in \mathcal{C}, \\ \infty, & \text{if } u \notin \mathcal{C}. \end{cases}$$

The normal cone $\mathcal{N}_{\mathcal{C}} x$ of $\mathcal{C}$ at x is defined by

$$\mathcal{N}_{\mathcal{C}} x = \{w \in \mathcal{H} : \langle w, y - x\rangle \leqslant 0,\ \forall y \in \mathcal{C}\}.$$

Then, $\iota_{\mathcal{C}}$ is a proper, lower semicontinuous, and convex function on $\mathcal{H}$ (see [1, 45]). Its subdifferential $\partial \iota_{\mathcal{C}}$ is a maximal monotone operator. Consequently, for any $\alpha > 0$, the resolvent operator is defined by

$$\mathcal{J}_\alpha^{\partial \iota_{\mathcal{C}}} u = (I + \alpha \partial \iota_{\mathcal{C}})^{-1} u, \quad \text{for all } \ u \in \mathcal{H}.$$

Furthermore, it follows that

$$\begin{aligned} \partial \iota_{\mathcal{C}} u &= \{w \in \mathcal{H} : \iota_{\mathcal{C}} u + \langle w, v - u\rangle \leqslant \iota_{\mathcal{C}} v,\ \forall v \in \mathcal{H}\} \\ &= \{w \in \mathcal{H} : \langle w, v - u\rangle \leqslant 0,\ \forall v \in \mathcal{C}\} = \mathcal{N}_{\mathcal{C}} u, \quad \text{for all } u \in \mathcal{C}. \end{aligned}$$

Hence, for each $\alpha > 0$, the resolvent satisfies the equivalence:

$$\begin{aligned} x = \mathcal{J}_\alpha^{\partial \iota_{\mathcal{C}}} u &\iff u \in x + \alpha \partial \iota_{\mathcal{C}} x \\ &\iff u - x \in \alpha \mathcal{N}_{\mathcal{C}} u \\ &\iff \langle u - x, v - x\rangle \leqslant 0,\ \forall v \in \mathcal{C} \\ &\iff x = \mathcal{P}_{\mathcal{C}} u, \end{aligned}$$

where $\mathcal{P}_{\mathcal{C}}$ denotes the metric projection onto $\mathcal{C}$. Accordingly, we derive the following results.

Algorithm 4.1 (Multi-inertial proximal method)**.**
Initialization: Let $\mu_k \in (0, 2)$, $d_k \in (0, 1)$ and $\{\alpha_k\}_{k \in N}$ be a sequence in $(0, \infty)$. Fix an integer $b \in N$. For each $s \in \{1, 2, \ldots, b\}$, let $\{\theta_{s,k}\}_{k=1}^{\infty}$ be a sequence of non-negative real numbers. Let $u_{1-b}, u_{2-b}, \ldots, u_0, u_1 \in \mathcal{H}$. Let $\{u_k\}$ be defined by

$$\begin{cases} z_k = u_k + \sum_{s=1}^{b} \theta_{s,k}(u_{k-s+1} - u_{k-s}), \\ w_k = \mathcal{P}_{\mathcal{C}}(z_k - \lambda_k \mathcal{F}^*(I - \mathcal{P}_{\mathcal{Q}})\mathcal{F} z_k), \\ u_{k+1} = w_k - \beta_k \mathcal{F}^*(I - \mathcal{P}_{\mathcal{Q}})\mathcal{F} w_k, \end{cases}$$

where

$$\lambda_k = \frac{\mu_k \|(I - \mathcal{P}_{\mathcal{Q}})\mathcal{F} z_k\|^2}{\|\mathcal{F}^*(I - \mathcal{P}_{\mathcal{Q}})\mathcal{F} z_k\|^2 + d_k} \quad \text{and} \quad \beta_k = \frac{\mu_k \|(I - \mathcal{P}_{\mathcal{Q}})\mathcal{F} w_k\|^2}{\|\mathcal{F}^*(I - \mathcal{P}_{\mathcal{Q}})\mathcal{F} w_k\|^2 + d_k}.$$

Theorem 4.2. *Let* $\{u_k\}$ *be defined by Algorithm 4.1. For each* $s \in \{1, 2, \ldots, b\}$, *if* $\sum_{k=1}^{\infty} \theta_{s,k} < +\infty$, $\lim_{k\to\infty} d_k = 0$ *and* $0 < \liminf_{k\to\infty} \mu_k \leqslant \limsup_{k\to\infty} \mu_k < 0$, *then* $\{u_k\}$ *converges weakly to a point in* Γ.

In 2021, Shehu et al. [44] introduced an alternating inertial CQ method for solving split feasibility problems. They demonstrated the applicability of their results to signal processing, as well as to a real-world scenario involving a jointly constrained Nash equilibrium model. The Shehu et al. method is defined by the following iterative scheme:

Algorithm 4.3 (Alternated inertial CQ method)**.**
Initialization: Let $\{\mu_k\} \subset (0, 4)$ be non-decreasing and $\{\theta_k\} \subset [0, \infty)$ and $u_0, u_1 \in \mathcal{H}$

$$w_k = \begin{cases} u_k + \theta_k(u_k + u_{k-1}), & k = \text{odd}, \\ u_k, & k = \text{even}, \end{cases}$$

and $u_{k+1} = \mathcal{P}_{\mathcal{C}}(w_k - \lambda_k \mathcal{F}^*(I - \mathcal{P}_{\mathcal{Q}})\mathcal{F}w_k)$, where

$$\lambda_k = \frac{\mu_k \frac{1}{2}\|(I - \mathcal{P}_{\mathcal{Q}})\mathcal{F}w_k\|^2}{\|\mathcal{F}^*(I - \mathcal{P}_{\mathcal{Q}})\mathcal{F}w_k\|^2},$$

and $0 < \alpha \leqslant \mu_k(1 + \theta_k) \leqslant \beta < 4$.

4.2. Image restoration

In this section, we demonstrate the restoration of knee X-ray images [50] for osteoporosis using our proposed method (Algorithm 4.1) and compare the results with those obtained by Dong et al. method (Algorithm 1.2) and the Shehu method (Algorithm 4.3). All computations were carried out in MATLAB R2025A on an HP laptop with an Intel(R) Core(TM) i7-1165G7 processor and 16 GB of RAM.

Next, we consider the image recovery problem, which can be formulated by the following linear equation:

$$b = Dx + v, \tag{4.2}$$

where $b \in R^{M\times 1}$ is the observed (degraded) image, $D \in R^{M\times M}$ is a blurring matrix, $x \in R^{M\times 1}$ denotes the original image, and $v \in R^{M\times 1}$ is the noise component.

It is important to note that the model in (4.2) can be equivalently reformulated as the following convex optimization problem:

$$\min_{x\in R^M} \frac{1}{2}\|b - Dx\|_2^2.$$

We define $\mathcal{C} = [0, 255]^{M\times N}$ and $\mathcal{Q} = \{b\}$, then the least squares problem problem can be considered as the SFP Equation (4.1). To assess the quality of the restored images, we use two standard metrics: Peak Signal-to-Noise Ratio (PSNR) [47] and Structural Similarity Index Measure (SSIM) [49], defined as follows:

$$\text{PSNR} := 20\log_{10}\left(\frac{255^2}{\|x_r - x\|_2^2}\right), \quad \text{SSIM} := \frac{(2\theta_x\theta_{x_r} + c_1)(2\sigma_{xx_r} + c_2)}{(\theta_x^2 + \theta_{x_r}^2 + c_1)(\sigma_x^2 + \sigma_{x_r}^2 + c_2)},$$

where all parameter are defined as in earlier studies [47, 49]. In this example, the starting points u_{-4},u_{-3},u_{-2}, u_{-1}, u_0, and u_1 are initialized as the blurred image. The method parameters are set as follows.

- Algorithm 4.1: $\theta_{1,k} = \frac{1}{(10k^3 + k)^5}$, for $1 \leqslant k \leqslant 200$, set $t_1 = 1$, and define $\theta_{2,k} = \frac{t_k - 1}{t_{k+1}}$, where $t_{k+1} = \frac{1 + \sqrt{1 + 4t_k^2}}{2}$ and for $k > 200$, set $\theta_{2,k} = \frac{1}{(4k+1)^2}$, $\theta_{3,k} = \frac{1}{(3k+1)^4}$, $\theta_{4,k}, \theta_{5,k} = \frac{1}{(100k+1)^7}$, $\beta_k = \frac{1}{(k+1)^2}$, $d_k = \frac{0.01k}{k+1}$, $\lambda_1 = 0.5$, and $\mu = 1.2$;

- Dong et al. [18]: $\theta_{1,k} = \frac{1}{(k+1)^2}$, $\theta_{2,k} = \frac{1}{(2k+1)^3}$, $\theta_{3,k} = \frac{1}{4k^5+1}$, $\eta_{1,k} = \frac{1}{(3k+1)^2}$, $\eta_{2,k} = \frac{1}{(5k+1)^2}$, $\eta_{3,k} = \frac{1}{k^2+1}$, $\lambda = \frac{1.9}{\|D\|^2}$, and $\alpha = 0.99$;
- Shehu et al. [44]: $\theta_k = 1.5$, $\lambda = 1$, and $\mu = 1$.

To simulate image degradation, three types of blur are applied to the original Knee X-ray image [50], as illustrated in Figure 1. The specific parameters used for each blur type are as follows.

1. out-of-focus blur (disk type): a disk-shaped blur with a radius of 6;
2. Gaussian blur: a Gaussian filter of size 7×7 with a standard deviation of 8;
3. motion blur: a linear motion blur with a length of 28 pixels and an angle of 181 degrees.

Figure 1: Knee X-ray image (size 545×662) [50].

In the following sections, we present the deblurred images obtained after 500 iterations for each method, as shown in Figures 1, 2, and 3. Furthermore, the restoration performance of each algorithm is evaluated using PSNR and SSIM metrics, which quantify the similarity between the restored and original images. A summary of the numerical results is provided in Table 1, with graphical comparisons shown in Figures 4 and 5.

Table 1: Numerical comparison of different inertial and other algorithm.

Method	disk		Gaussian		motion	
	PSNR	SSIM	PSNR	SSIM	PSNR	SSIM
Algorithm 4.1						
- 1 inertial	37.8016	0.9462	44.3561	0.9856	39.7120	0.9667
- 2 inertial	45.2013	0.9805	51.4512	0.9959	43.0399	0.9767
- 3 inertial	45.4083	0.9813	51.5470	0.9960	44.7641	0.9830
- 4 inertial	45.4083	0.9813	51.5470	0.9960	44.7641	0.9830
- 5 inertial	45.4083	0.9813	51.5470	0.9960	44.7641	0.9830
Dong et al.	34.2909	0.9252	42.2118	0.9677	33.6732	0.9210
Shehu et al.	36.2787	0.9413	42.2118	0.9773	34.7172	0.9304

As shown in Table 1, the proposed Algorithm 4.1 outperforms the methods of Dong et al. and Shehu et al. methods in restoring images degraded by different types of blurring. This advantage is particularly noticeable when using the multi-inertial term technique. Notably, when employing three or more inertial terms, the PSNR and SSIM values become consistently high and stable—for example, PSNR of 51.5470

and SSIM of 0.9960 for Gaussian blur, and PSNR of 44.7641 and SSIM of 0.9830 for motion blur. These results suggest that adding more than three inertial terms does not yield significant further improvement in performance, but rather enhances the stability of the outcomes. It is important to note that these results depend on the specific parameter configurations used in each method. Any variation in these parameters could potentially affect the accuracy and stability of the results.

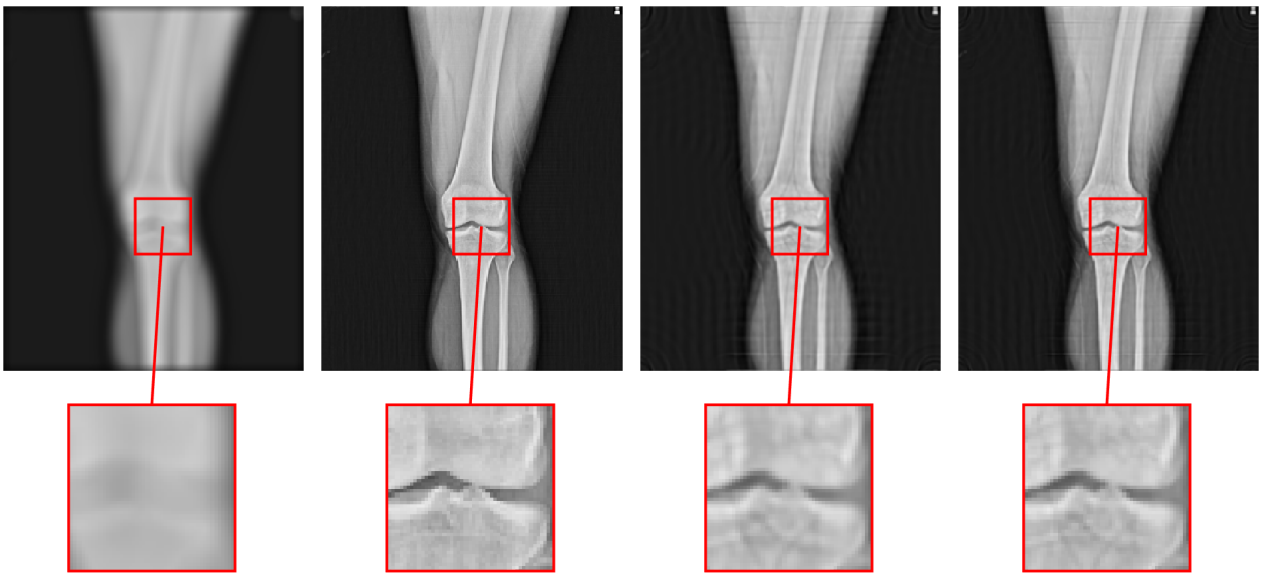

(a) Disk blur **(b)** Proposed **(c)** Dong et al. **(d)** Shehu et al.

Figure 2: The blurred image with disk and deblurred images.

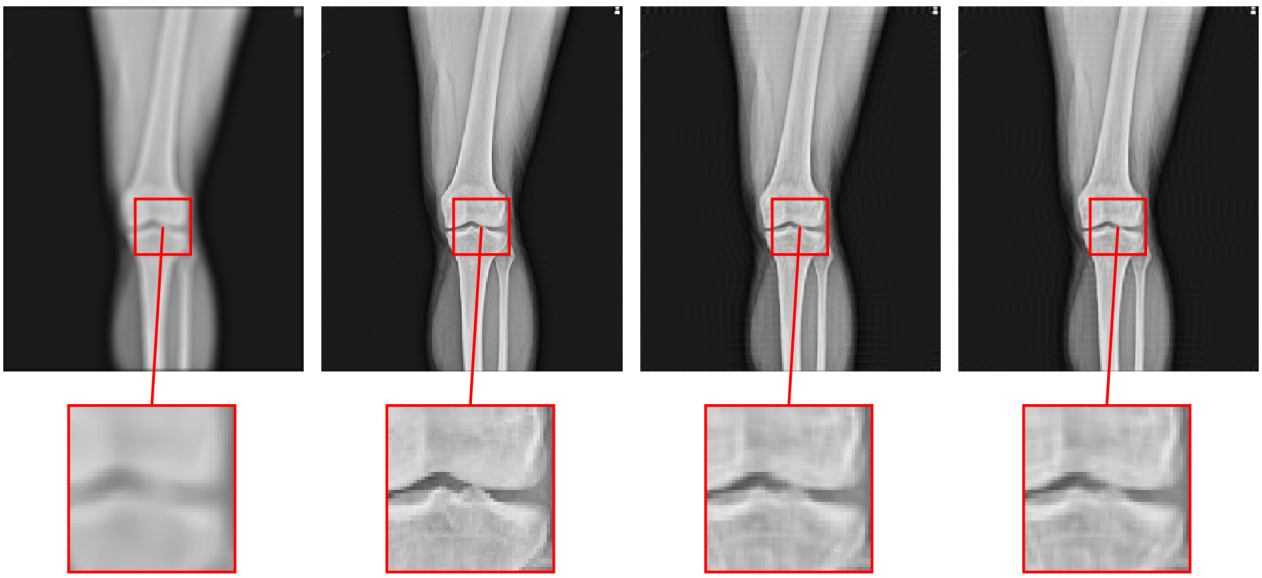

(a) Gaussian blur **(b)** Proposed **(c)** Dong et al. **(d)** Shehu et al.

Figure 3: The blurred image with Gaussian and deblurred images.

Figure 5 illustrates that the proposed method achieves higher and more stable PSNR and SSIM values when using three or more inertial terms, compared to using only one or two inertial terms. Notably, after approximately 250 iterations, both metrics become steady and consistent. This suggests that while increasing the number of inertial terms beyond three does not significantly enhance performance, it contributes to greater stability of results.

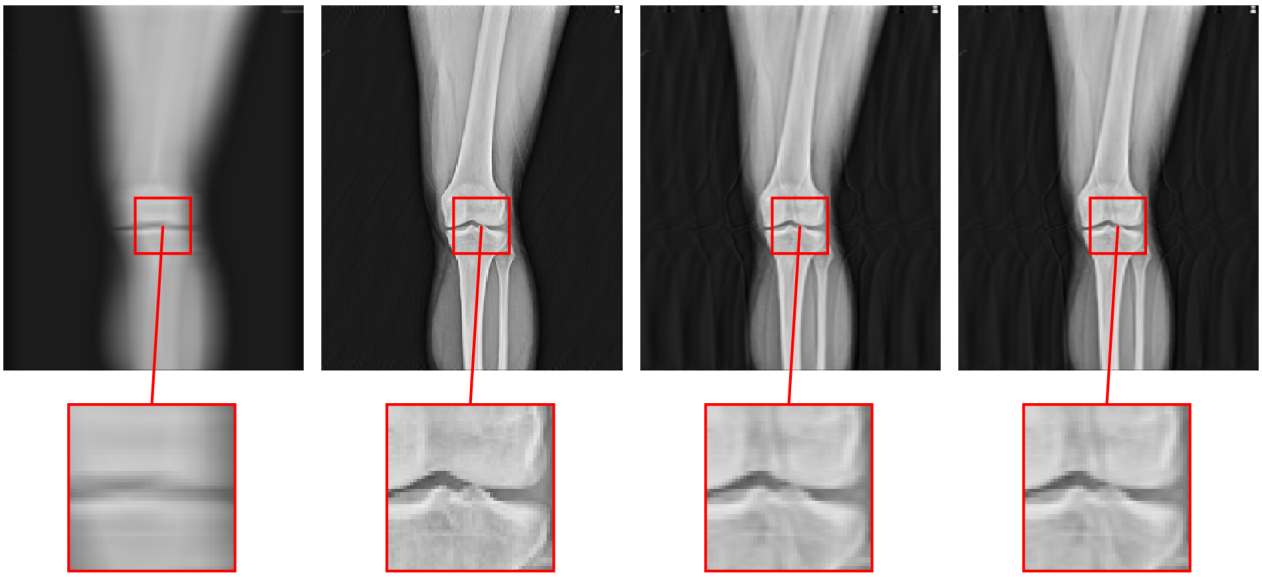

(a) Motion blur **(b)** Proposed **(c)** Dong et al. **(d)** Shehu et al.

Figure 4: The blurred image with motion and deblurred images.

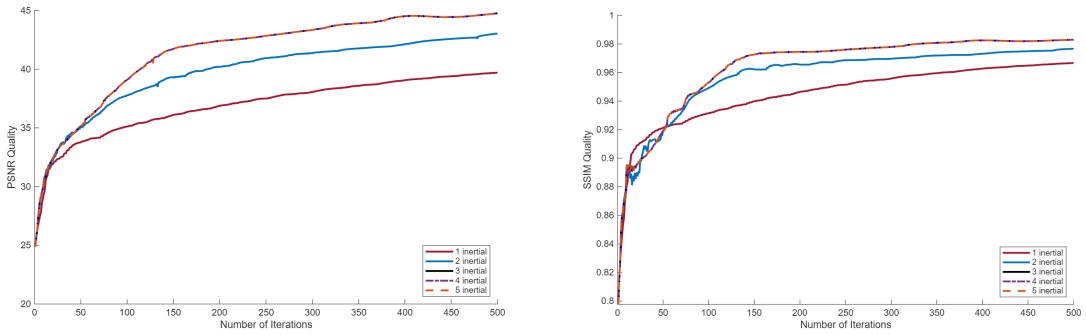

(a) PSNR **(b)** SSIM

Figure 5: PSNR and SSIM of proposed method by motion blur.

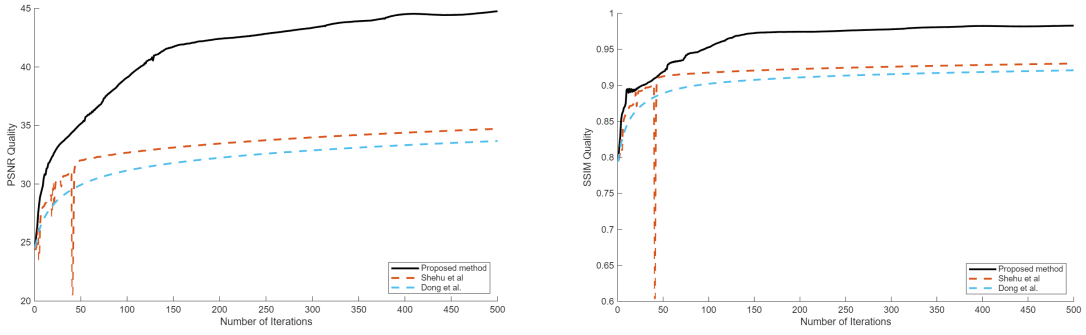

(a) PSNR **(b)** SSIM

Figure 6: PSNR and SSIM of each method by motion blur.

Figure 6 shows that the proposed method (using 3 inertial terms) outperforms the methods of Dong et al. and Shehu et al. in motion blur restoration. It achieves both higher PSNR and SSIM values and demonstrates a faster convergence rate. Particularly during the early iterations (within 100 steps), the proposed method rapidly improves image quality and stabilizes effectively, while the other methods plateau at lower quality levels. These findings highlight the effectiveness of the multi-inertial technique in enhancing both convergence speed and restoration quality under conditions of motion blur.

4.3. Data classification

In this section, we apply using our proposed method (Algorithm 4.1) to the data classification problem in the prediction of lung cancer. Lung cancer is one of the leading causes of cancer-related death worldwide, and early prediction plays a crucial role in improving patient outcomes. Lung cancer may be caused by genetic factors, environmental pollution, smoking, occupational hazards, and several lifestyle factors, manifested through various symptoms such as coughing, shortness of breath, chest pain, and fatigue.

In particular, we apply the extreme learning machine (ELM) to predict whether an individual is at risk of lung cancer based on multiple clinical and behavioral attributes. The predictive performance of the proposed model is also compared with conventional machine learning algorithms. The data sett used in this study contains 1,000 observations, 23 input attributes (shown in Table 2), and an output class with 3 levels [21].

Let us consider a training set $\{(x_n, y_n) : x_n \in R^N, y_n \in R^M, n = 1, 2, \ldots, W\}$, where each input x_n corresponds to a feature vector, and y_n denotes the associated class label. In the ELM model with a single hidden layer, the activation output at the i-th hidden node for an input x is expressed as $h_i(x) = U(\langle a_i, x\rangle + b_i)$, where U denotes the activation function, and a_i, b_i represent the input weight and bias of the i-th hidden unit, respectively.

The output of a single-hidden layer feedforward neural network is expressed as a linear combination of the responses from the hidden nodes:

$$R_n = \sum_{i=1}^{L} \omega_i h_i(x_n),$$

where ω_i denotes the output weight associated with the i-th hidden node, and L is the total number of hidden units. We define the hidden layer output matrix $A \in R^{W\times L}$ by

$$A = \begin{bmatrix} U(\langle a_1, x_1\rangle + b_1) & \cdots & U(\langle a_L, x_1\rangle + b_L) \\ \vdots & \ddots & \vdots \\ U(\langle a_1, x_W\rangle + b_1) & \cdots & U(\langle a_L, x_W\rangle + b_L) \end{bmatrix}.$$

Let A denote the hidden layer output matrix and $\Gamma = [t_1, t_2, \ldots, t_W]^T$ represents the target label vector derived from the training data. The output weight vector is denoted by $\omega = [\omega_1, \omega_2, \ldots, \omega_L]^T$. This weight vector can be computed via the closed form solution $\omega = A^\dagger\Gamma$, where $A^\dagger$ denotes the Moore-Penrose generalized inverse of A. However, directly computing $A^\dagger$ is often impractical, especially when A is ill-conditioned or singular. To address this issue, we consider a convex optimization approach to estimating ω. Least squares minimization is commonly employed in this context to obtain a stable solution. The least squares formulation is given by

$$\min_{\omega\in R^L} \frac{1}{2}\|A\omega - \Gamma\|_2^2.$$

To evaluate the performance of the classification model, we employ four standard evaluation metrics: accuracy, precision, recall, and F1-score. These metrics are widely used in binary classification tasks and are defined as follows:

- Accuracy measures the proportion of correctly predicted instances among all predictions:

$$\text{Accuracy} = \frac{TP + TN}{TP + TN + FP + FN} \times 100\%.$$

- Precision quantifies the proportion of true positive predictions among all positive predictions:

$$\text{Precision} = \frac{TP}{TP + FP} \times 100\%.$$

- Recall (also known as sensitivity or true positive rate) evaluates the proportion of actual positives correctly identified:

$$\text{Recall} = \frac{\text{TP}}{\text{TP} + \text{FN}} \times 100\%.$$

- F1-score is the harmonic mean of precision and recall, which balances both measures:

$$\text{F1-score} = \frac{2 \times (\text{Precision} \times \text{Recall})}{\text{Precision} + \text{Recall}}.$$

In these definitions, TP (True Positives), TN (True Negatives), FP (False Positives), and FN (False Negatives) are derived from the confusion matrix, which compares the predicted and actual class labels. For multi-class classification tasks, we employ the categorical cross-entropy loss to evaluate the model's predictive performance. This loss function is defined as:

$$\text{loss} = -\frac{1}{N} \sum_{n=1}^{N} \sum_{c=1}^{C} s_{n,c} \log(\hat{s}_{n,c}),$$

where $\hat{s}_{n,c}$ and $s_{n,c}$ denote the predicted probability and the corresponding ground truth indicator for the c-th class of the n-th instance, respectively. The total number of training instances is represented by N, and the number of output classes is defined by C.

The dataset was randomly divided into a training set (80%) and a testing set (20%) using stratified sampling, thereby preserving the class distribution and enabling a fair evaluation of the classification performance. Table 3 shows the number of instances in each class for both training and testing sets.

Table 2: Descriptive statistics of features

Feature	**Mean**	**Std**	**Min**	**Max**
age	37.174	12.005	14.000	73.000
gender	1.402	0.491	1.000	2.000
air pollution	3.840	2.030	1.000	8.000
alcohol use	4.563	2.620	1.000	8.000
dust allergy	5.165	1.981	1.000	8.000
occupational hazards	4.840	2.108	1.000	8.000
genetic risk	4.580	2.127	1.000	8.000
chronic lung disease	4.380	1.849	1.000	7.000
balanced diet	4.491	2.136	1.000	8.000
obesity	4.465	2.125	1.000	8.000
smoking	3.948	2.496	1.000	8.000
passive smoker	4.195	2.312	1.000	8.000
chest pain	4.438	2.280	1.000	8.000
coughing of blood	4.859	2.428	1.000	9.000
fatigue	3.856	2.245	1.000	9.000
weight loss	3.855	2.207	1.000	9.000
shortness of breath	4.240	2.285	1.000	9.000
wheezing	3.777	2.230	1.000	8.000
swallowing difficulty	3.746	2.270	1.000	9.000
clubbing of finger nails	3.923	2.388	1.000	9.000
frequent cold	3.536	1.833	1.000	7.000
dry cough	3.853	2.039	1.000	7.000
snoring	2.926	1.475	1.000	7.000

Std: Standard deviation

Table 3: Class distribution in training and testing sets.

Class	Train Count	Test Count	Total
Low	242	61	303
Medium	266	66	332
High	292	73	365

Model parameters were configured with a fixed setup to allow a consistent comparison of algorithmic performance. The computational setup is based on ELM framework, where the activation function is set as the sigmoid function. The number of hidden nodes is set to $L = 180$, with the input weights a_i randomly initialized in the range $[-2, 2]$, and the biases b_i drawn from the range $[-4, 4]$.

For evaluation purposes, we compare the proposed method with two baseline approaches referred to as Dong et al. [18] and Shehu et al. [44]. The initial inertial vectors are specified as u_{-2}, u_{-1}, $u_0 = (1, 1, \ldots, 1), u_1 = (0, 0, \ldots, 0)$. The detailed parameter settings for each algorithm used in the comparison are listed below:

1. Algorithm 4.1 with 3 inertial: $\theta_{1,k} = \dfrac{1}{(20k+1)^2}$, $\theta_{2,k} = \dfrac{1}{(40k+1)^3}$, $\theta_{3,k} = \dfrac{1}{(30k+1)^4}$, $\beta_k = \dfrac{1}{(k+1)^2}$, $d_k = \dfrac{0.01k}{k+1}$, $\lambda_1 = 0.5$, and $\mu = 0.01$;
2. Dong et al. [18]: $\theta_{1,k} = \frac{1}{(k+1)^2}$, $\theta_{2,k} = \frac{1}{(2k+1)^3}$, $\theta_{3,k} = \frac{1}{4k^5+1}$, $\eta_{1,k} = \frac{1}{(k)^2}$, $\eta_{2,k} = \frac{1}{(2k^2+1)}$, $\eta_{3,k} = \frac{1}{5k^2+1}$, $\lambda = \frac{1}{\|A\|^2}$, and $\alpha = 0.5$;
3. Shehu et al. [44]: $\theta_k = 1.5$, $\lambda = 1$, and $\mu = 1$.

The performance of each algorithm was evaluated over 1000 iterations. The corresponding numerical results are summarized in Table 4. As shown in the table, each algorithm achieves its best performance at the 1000th iteration. Table 4 demonstrates the performance of each algorithm after 1000 iterations. The

Table 4: The performance of each algorithm for 1000 iterations.

	Shehu et al.	Dong et al.	Algorithm 4.1
Accuracy train	94.7500	97.9167	**98.6667**
Accuracy test	94.6667	97.3333	**98.0000**
Precision	92	96	**97**
Recall	92	96	**97**
F1-Score	92	96	**97**
Loss test	0.2255	0.2032	**0.1927**
Loss train	0.2241	0.2021	**0.1920**
Time (s)	3.1669	5.0376	**3.0015**

proposed Algorithm 4.1 achieves the highest classification performance, with a testing accuracy of 98.00%, outperforming both Shehu et al. and Dong et al. in all evaluation metrics including precision, recall, F1-score, and loss values. Furthermore, Algorithm 4.1 exhibits a shorter time, indicating its efficiency and suitability for practical applications.

Figure 7 shown the training and testing accuracy of Algorithm 4.1 across 1000 iterations. The accuracy improves rapidly during the early iterations and gradually stabilizes, eventually reaching values to 98% for both training and validation. Similarly, Figure 8 shows a steady decrease in the training and testing loss, indicating convergence of the model. The small gap between training and validation curves in both plots suggests that the algorithm generalizes well without overfitting.

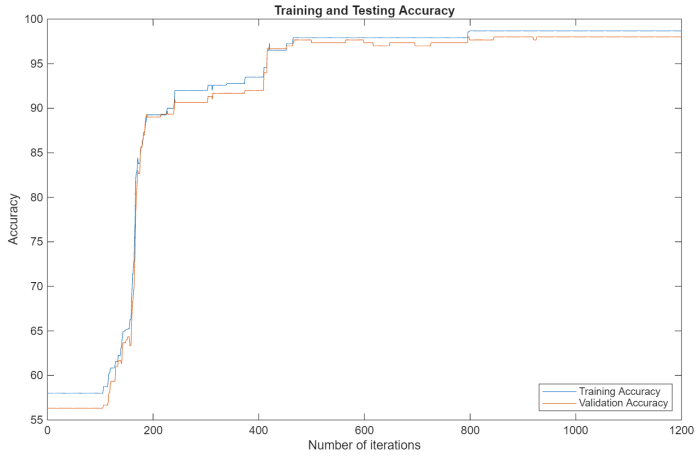

Figure 7: Accuracy of Algorithm 4.1.

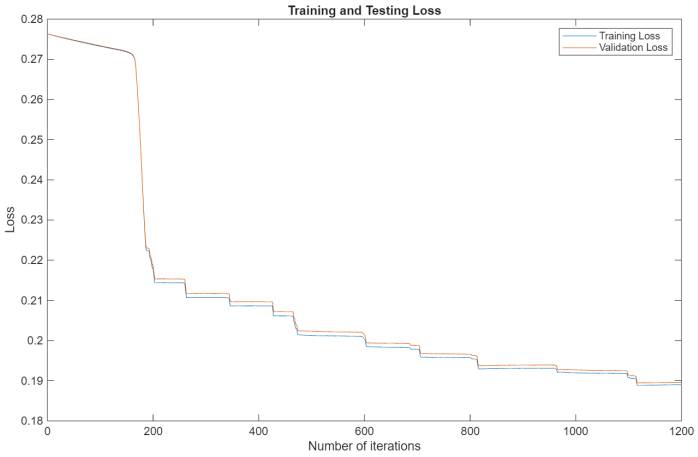

Figure 8: Loss of Algorithm 4.1.

5. Conclusion

In this work, we propose an efficient method that integrates multi-inertial extrapolation with a self-adaptive stepsize technique to solve split variational inclusion problems in Hilbert spaces. Theoretical analysis guarantees weak convergence under mild conditions. Numerical experiments-particularly in image deblurring and data classification-demonstrate that employing three or more inertial terms notably improves both the stability and convergence speed of the algorithm. Furthermore, these advantages are achieved without the need for strict parameter tuning, demonstrating the method's reliability.

Authors' contributions

Suparat Kesornprom: formal analysis, software, data curation, visualization, writing-original draft.

Papatsara Inkrong: formal analysis, software, data curation, writing-original draft.

Papinwich Paimsang: validation, software, writing-original draft. **Nattawut Pholasa:** Visualization, resources, writing-review and editing.

Prasit Cholamjiak: conceptualization, writing-review and editing, supervision.

Acknowledgments

We would like to thank you for following the instructions above very closely in advance. It will definitely save us lot of time and expedite the process of your paper's publication. This research was partially supported by Chiang Mai University and Fundamental Fund 2025, Chiang Mai University, Chiang Mai, Thailand. Nattawut Pholasa was supported by University of Phayao and Thailand Science Research and Innovation Fund (Fundamental Fund 2025, Grant No. 5120/2567).

Data availability

The dataset used in this research is publicly available at https://www.kaggle.com/code/guslovesmath/lung-cancer-ml-classification/input.

References

[1] R. P. Agarwal, D. O'Regan, D. R. Sahu, *Fixed point theory for Lipschitzian-type mappings with applications*, Springer, New York, (2009). 4.1
[2] F. Alvarez, *Weak convergence of a relaxed and inertial hybrid projection-proximal point algorithm for maximal monotone operators in Hilbert space*, SIAM J. Optim., **14** (2004), 773–782. 1, 1
[3] F. Alvarez, H. Attouch, *An inertial proximal method for maximal monotone operators via discretization of a nonlinear oscillator with damping*, Set-Valued Anal., **9** (2001), 3–11. 1
[4] H. H. Bauschke, P. L. Combettes, *Convex analysis and monotone operator theory in Hilbert spaces*, Springer, New York, (2011). 2.2
[5] R. I. Boţ, E. R. Csetnek, *An inertial alternating direction method of multipliers*, Minimax Theory Appl., **1** (2016), 29–49. 1
[6] C. Byrne, *Iterative oblique projection onto convex sets and the split feasibility problem*, Inverse Probl., **18** (2002), 441–453. 1
[7] C. Byrne, *A unified treatment of some iterative algorithms in signal processing and image reconstruction*, Inverse Probl., **20** (2004), 103–120. 1
[8] C. Byrne, Y. Censor, A. Gibali, S. Reich, *The split common null point problem*, J. Nonlinear Convex Anal., **13** (2012), 759–775. 1, 1
[9] A. Cegielski, *General method for solving the split common fixed point problem*, J. Optim. Theory Appl., **165** (2015), 385–404. 1
[10] Y. Censor, T. Bortfeld, B. Martin, A. Trofimov, *A unified approach for inversion problems in intensity-modulated radiation therapy*, Phys. Med. Biol., **51** (2006). 1
[11] Y. Censor, A. Gibali, S. Reich, *Algorithms for the split variational inequality problem*, Numer. Algorithms, **59** (2012), 301–323. 1
[12] Y. Censor, A. Segal, *The split common fixed point problem for directed operators*, J. Convex Anal., **16** (2009), 587–600. 1
[13] C. Chen, R. H. Chan, S. Ma, J. Yang, *Inertial proximal ADMM for linearly constrained separable convex optimization*, SIAM J. Imaging Sci., **8** (2015), 2239–2267. 1
[14] C.-S. Chuang, *Strong convergence theorems for the split variational inclusion problem in Hilbert spaces*, Fixed Point Theory Appl., **2013** (2013), 20 pages. 2.3, 2.4, 2.5
[15] C.-S. Chuang, *Hybrid inertial proximal algorithm for the split variational inclusion problem in Hilbert spaces with applications*, Optimization, **66** (2017), 777–792. 1
[16] P. L. Combettes, L. E. Glaudin, *Quasi-nonexpansive iterations on the affine hull of orbits: from Mann's mean value algorithm to inertial methods*, SIAM J. Optim., **27** (2017), 2356–2380. 1
[17] Y. Dang, Y. Gao, *The strong convergence of a KM-CQ-like algorithm for a split feasibility problem*, Inverse Probl., **27** (2010), 9 pages. 1
[18] Q. L. Dong, J. Z. Huang, X. H. Li, Y. J. Cho, T. M. Rassias, *MiKM: multi-step inertial Krasnosel'skiĭ–Mann algorithm and its applications*, J. Global Optim., **73** (2019), 801–824. 1, 1, ?, 4.3, 2
[19] K. Goebel, W. A. Kirk, *Topics in metric fixed point theory*, Cambridge University Press, Cambridge, (1990). 2.1
[20] K. Goebel, S. Reich, *Uniform convexity, hyperbolic geometry, and nonexpansive mappings*, Marcel Dekker, New York, (1984). ?
[21] Guslovesmath, *Lung Cancer ML Classification (Kaggle Notebook)*, https://www.kaggle.com/code/guslovesmath/lung-cancer-ml-classification/input (Accessed 12 June 2025) 4.3
[22] A. Hadjian, S. Heidarkhani, *Existence of one non-trivial anti-periodic solution for second-order impulsive differential inclusions*, Math. Methods Appl. Sci., **40** (2017), 5009–5017. 1
[23] S. Heidarkhani, G. A. Afrouzi, A. Hadjian, J. Henderson, *Existence of infinitely many anti-periodic solutions for second-order impulsive differential inclusions*, Electron. J. Differ. Equ., **2013** (2013), 13 pages. 1

[24] P. Inkrong, P. Cholamjiak, *Modified proximal gradient methods involving double inertial extrapolations for monotone inclusion*, Math. Methods Appl. Sci., **47** (2024), 12132–12148. 1
[25] P. Inkrong, P. Cholamjiak, *On multi-inertial extrapolations and forward-backward-forward algorithms*, Carpathian J. Math., **40** (2024), 293–305. 2.6
[26] P. Inkrong, P. Paimsang, P. Cholamjiak, *A recent fixed point method based on two inertial terms*, J. Anal., **33** (2025), 521–535. 1
[27] O. S. Iyiola, Y. Shehu, *Convergence results of two-step inertial proximal point algorithm*, Appl. Numer. Math., **182** (2022), 57–75. 1
[28] K. Kankam, W. Cholamjiak, P. Cholamjiak, J.-C. Yao, *Enhanced proximal gradient methods with multi inertial terms for minimization problem*, J. Appl. Math. Comput., (2025), 1–39. 1
[29] X. Li, Q.-L. Dong, A. Gibali, *PMiCA-Parallel multi-step inertial contracting algorithm for solving common variational inclusions*, J. Nonlinear Funct. Anal., **2022** (2022), 12 pages. 1
[30] J. Liang, *Convergence rates of first-order operator splitting methods*, Doctoral Dissertation, Normandie Université; GREYC CNRS UMR 6072, (2016). 1
[31] G. Marino, H.-K. Xu, *Convergence of generalized proximal point algorithms*, Commun. Pure Appl. Anal., **3** (2004), 791–808. 2.3
[32] A. Moudafi, *Split monotone variational inclusions*, J. Optim. Theory Appl., **150** (2011), 275–283. 1
[33] T. L. N. Nguyen, Y. Shin, *Deterministic sensing matrices in compressive sensing: A survey*, Sci. World J., **2013** (2013), 6 pages. 1
[34] Z. Opial, *Weak convergence of the sequence of successive approximations for nonexpansive mappings*, Bull. Amer. Math. Soc., **73** (1967), 591–597. 2.8
[35] M. O. Osilike, S. C. Aniagbosor, *Weak and strong convergence theorems for fixed points of asymptotically nonexpansive mappings*, Math. Comput. Model., **32** (2000), 1181–1191. 2.7
[36] N. Pakkaranang, P. Kumam, Y. I. Suleiman, B. Ali, *Bounded perturbation resilience of viscosity proximal algorithm for solving split variational inclusion problems with applications to compressed sensing and image recovery*, Math. Methods Appl. Sci., **45** (2022), 4085–4107. 1
[37] B. T. Polyak, *Some methods of speeding up the convergence of iterates methods*, USSR Comput. Math. Math. Phys., **4** (1964), 1–17. 1
[38] B. T. Polyak, *Introduction to Optimization*, Optimization Software, Publications Division, New York, (1987). 1
[39] C. Poon, J. Liang, *Trajectory of alternating direction method of multipliers and adaptive acceleration*, Adv. Neural Inf. Process. Syst., **32** (2019). 1
[40] S. Reich, *Extension problems for accretive sets in Banach spaces*, J. Funct. Anal., **26** (1977), 378–395. 2.3
[41] S. Reich, T. M. Tuyen, *Cyclic projection methods for solving the split common zero point problem in Banach spaces*, Fixed Point Theory, **25** (2024), 353–370. 1
[42] S. Reich, T. M. Tuyen, *Two new selfadaptive algorithms for solving the split feasibility problem in Hilbert space*, Numer. Algorithms, **95** (2024), 1011–1032. 1
[43] S. Reich, T. M. Tuyen, *Three shrinking projection methods with multiple inertial effects for solving a class of split feasibility problems*, J. Fixed Point Theory Appl., **26** (2024), 19 pages. 1
[44] Y. Shehu, Q.-L. Dong, L.-L. Liu, *Global and linear convergence of alternated inertial methods for split feasibility problems*, Rev. R. Acad. Cienc. Exactas Fís. Nat. Ser. A Mat. RACSAM, **115** (2021), 26 pages. 4.1, ?, 4.3, 3
[45] L. Shulman, *Knowledge and teaching: Foundations of the new reform*, Harv. Educ. Rev., **57** (1987), 1–23. 4.1
[46] D. V. Thong, S. Reich, X.-H. Li, P. T. H. Tham, *An efficient algorithm with double inertial steps for solving split common fixed point problems and an application to signal processing*, Comput. Appl. Math., **44** (2025), 17 pages. 1
[47] K.-H. Thung, P. Raveendran, *A survey of image quality measures*, In: 2009 International Conference for Technical Postgraduates (TECHPOS), IEEE, (2009), 1–4. 4.2
[48] N. Wairojjana, N. Pholasa, N. Pakkaranang, *On strong convergence theorems for a viscosity-type Tseng's extragradient methods solving quasimonotone variational inequalities*, Nonlinear Funct. Anal. Appl., **27** (2022), 381–403. 1
[49] Z. Wang, A. C. Bovik, H. R. Sheikh, E. P. Simoncelli, *Image quality assessment: from error visibility to structural similarity*, IEEE Trans. Image Process., **13** (2004), 600–612. 4.2
[50] Orvile, *Knee X-ray Osteoporosis Database [Data set]*, Kaggle, (2022). 4.2, 4.2, 1
[51] H.-K. Xu, *Iterative methods for the split feasibility problem in infinite-dimensional Hilbert spaces*, Inverse Probl., **26** (2010), 17 pages. 1
[52] C. Zhang, Q.-L. Dong, J. Chen, *Multi-step inertial proximal contraction algorithms for monotone variational inclusion problems*, Carpathian J. Math., **36** (2020), 159–177. 1
[53] C. Zong, G. Zhang, Y. Tang, *Multi-step inertial forward-backward-half forward algorithm for solving monotone inclusion*, Linear Multilinear Algebra, **71** (2023), 631–661. 1